

Loss of the Zymogen Granule Protein Syncollin Affects Pancreatic Protein Synthesis and Transport but Not Secretion

Wolfram Antonin,¹ Martin Wagner,^{2†} Dietmar Riedel,¹ Nils Brose,³ and Reinhard Jahn^{1*}

Departments of Neurobiology¹ and Molecular Cell Biology,² Max Planck Institute for Biophysical Chemistry 37077 Göttingen, and Department of Molecular Neurobiology, Max Planck Institute for Experimental Medicine, 37075 Göttingen,³ Germany

Received 20 September 2001/Returned for modification 29 October 2001/Accepted 4 December 2001

Syncollin is a small protein that is abundantly expressed in pancreatic acinar cells and that is tightly associated with the luminal side of the zymogen granule membrane. To shed light on the hitherto unknown function of syncollin, we have generated syncollin-deficient mice. The mice are viable and show a normal pancreatic morphology as well as normal release kinetics in response to secretagogue stimulation. Although syncollin is highly enriched in zymogen granules, no change was found in the overall protein content and in the levels of chymotrypsin, trypsin, and amylase. However, syncollin-deficient mice reacted to caerulein hyperstimulation with a more severe pancreatitis. Furthermore, the rates of both protein synthesis and intracellular transport of secretory proteins were reduced. We conclude that syncollin plays a role in maturation and/or concentration of zymogens in zymogen granules.

The exocrine pancreas is specialized for the synthesis, storage, and release of digestive proenzymes. Since the pancreas exhibits the highest rate of protein synthesis among all mammalian tissues (8), it has served for many years as the model system for the study of intracellular protein transport and secretion (31). In pancreatic acinar cells, secretory proteins are synthesized at the rough endoplasmic reticulum and transported to the Golgi apparatus. In the *trans*-Golgi network, proteins are segregated into condensing vacuoles that undergo further maturation to zymogen granules (for a review, see reference 37). During maturation and condensation, granular content proteins are segregated from proteins destined for constitutive secretion (for a review, see references 3 and 43). Mature granules are stored in the apical pole of the acinar cell. Upon nervous or hormonal stimulation, a selective rise in the local Ca²⁺ concentration is observed in the apical pole, which triggers exocytotic discharge of the granule content into the pancreatic duct (32).

Formation, maturation, and exocytosis of zymogen granules are multistep processes that are only incompletely understood at the molecular level. For instance, it is largely unknown how zymogens are sorted in the *trans*-Golgi network and how they are packaged and concentrated in zymogen granules. Furthermore, the molecular steps involved in granule docking and fusion still need to be elucidated. As in many other intracellular fusion events, members of the Rab and SNARE (for soluble *N*-ethylmaleimide sensitive factor attachment protein receptor) protein families were shown to be involved in pancreatic secretion (16, 18, 29, 30, 44), but how they are regulated and which proteins are involved in transmitting the calcium signal to the exocytotic machinery are still unknown.

To shed light on the mechanisms involved in granule maturation and fusion, a better understanding of the components of the granule membrane is needed. Granule membrane constituents are likely to be essential for acinar cell function for two reasons. First, protein sorting and packaging will, at least to some extent, depend on interactions between content and membrane components. Second, the granule membrane must contain trafficking proteins to ensure functioning of the zymogen granule as a trafficking organelle. Membrane proteins likely to be involved in trafficking include the SNAREs synaptobrevin 2 (17) and syntaxin 3 (15), the Rab proteins Rab3D (28, 45), Rab4 (29), and Rab5 (46), and secretory carrier membrane proteins (SCAMP) (7). Membrane proteins involved in sorting and packaging of zymogens need to have their functional domains exposed on the luminal side of the granule membrane. Examples for such proteins include ZG16 (10), GP-300 (11), and GP-2 (21, 35).

Recently we have identified a novel protein, termed syncollin, as a major constituent of the zymogen granule membrane (13). Syncollin was isolated by virtue of its ability to bind to syntaxins 1 and 2. Binding was reduced at increasing calcium concentrations. Interestingly, the protein is strongly expressed in the pancreas, whereas it is either absent or expressed at very low levels in other secretory tissues. Furthermore, the addition of recombinant syncollin to a cell-free assay for exocytosis inhibited the reaction, suggesting that the protein may play a role in regulating exocytosis. However, it has recently become clear that the protein carries a signal sequence and that it is localized to the luminal surface of the granule membrane (2). These findings are difficult to reconcile with a role of syncollin in membrane trafficking. Thus, the function of syncollin in the pancreatic acinar cell has remained unclear.

To analyze the function of syncollin, we have now generated syncollin-deficient mice. These mice are viable and fertile and show no obvious defects. However, the pancreas of syncollin-deficient mice is more susceptible to hyperstimulation by caerulein *in vivo*. Furthermore, acinar cells from these mice display reduced rates of protein synthesis and intracellular

* Corresponding author. Mailing address: Department of Neurobiology, Max Planck Institute for Biophysical Chemistry, Am Fassberg 11, 37077 Göttingen, Germany. Phone: 49-551 201 1634. Fax: 49-551 201 1639. E-mail: rjahn@gwdg.de.

† Present address: Department of Gastroenterology and Endocrinology, University of Ulm, 89081 Ulm, Germany.

transport *in vitro*, although no change was found in the zymogen content of the organ and in the kinetics of secretagogue-induced release. We conclude that syncollin, while not being essential for acinar cell function, plays a role in efficient maturation and/or concentration of zymogens.

MATERIALS AND METHODS

Caerulein was purchased from Pharmacia (Erlangen, Germany). Monoclonal antibodies specific for syncollin (Cl 87.1 [2]), synaptobrevin 2 (Cl 69.1 [12]), and GDP dissociation inhibitor (Cl 81.1 [9]) as well as polyclonal antibodies specific for syntaxin 4 (18) were described previously and are commercially available from Synaptic Systems (Göttingen, Germany). A monoclonal antibody specific for rabphilin (clone Cl76.2; subclass immunoglobulin M) was raised against recombinant rabphilin using standard procedures (24). A rabbit serum specific for Rab3D (no cross-reactivity towards other Rab3 isoforms) was raised against a synthetic peptide and will be described in detail elsewhere (D. Riedel et al., unpublished data).

Rabbit polyclonal antibodies specific for syntaxin 2 and syntaxin 3 were generated by immunization with the cytoplasmic domains of syntaxin 2 (residues 1 to 265) and syntaxin 3 (residues 1 to 260), respectively (14), and can be obtained from Synaptic Systems. Antibodies specific for SCAMP and β -tubulin were obtained from Synaptic Systems and Sigma, Deisenhofen, Germany, respectively. Antibodies specific for protein disulfide isomerase (PDI), calreticulin, and BiP were kind gifts of Nguyen Van (University Göttingen, Göttingen, Germany).

Generation of syncollin-deficient mice. Syncollin mutant mice were generated by homologous recombination in embryonic stem cells as described previously (39, 41). In short, two genomic clones containing both coding exons of murine syncollin were isolated from a λ FixIIISV129 mouse genomic library (Stratagene, La Jolla, Calif.) using standard techniques. The gene targeting vector based on these clones replaced the first exon of syncollin (amino acids 1 to 132) (see Fig. 1) with a neomycin resistance cassette. Following electroporation and selection, recombinant stem cells were analyzed by Southern blotting after digestion of DNA with *Pst*I. For hybridization, an outside probe localized 3' of the targeting vector short arm was used. Three positive clones were injected into mouse blastocysts to obtain highly chimeric mice that transmitted the mutation through the germ line. Germ line transmission was confirmed by Southern blotting. Subsequent genotyping was performed by PCR using primer pairs specific for wild-type allele (5'-ACTGGTCCGACTCCATCTCTGCCCTC and 5'-GTG CACTCAGAGATGGGACCTCCAGG) or mutant allele (5'-GAGCGGC GCGGCGGAGTTGTTGAC and 5'-GTGCACTCAGAGATGGGACCTC CAGG), both generating fragments of 210 bp. Mice were bred and maintained using standard mouse husbandry procedures. In all comparative experiments, we exclusively used sex-matched littermates and mice of both sexes.

Database searches. GenBank was searched for sequences derived from human syncollin by the use of BLAST (1) programs of the National Center for Biotechnology (Bethesda, Md.) with amino acid sequences of mouse and rat syncollin. Several expressed sequence tag clones were identified (#7293944, #8362822, #10582602, #2896277, and #5850967). From these, the human sequence was obtained and verified by comparison with the sequence of the human genome project (GenBank accession no. AC011443.6).

Light and electron microscopy. For light microscopy, pancreatic tissue of three individual animals from each genotype was fixed by immersion in 4% phosphate-buffered paraformaldehyde for 12 h, embedded in paraffin, and sectioned (4 μ m). Sections were stained with hematoxylin-eosin and examined with a photomicroscope (Zeiss, Oberkochen, Germany).

For transmission electron microscopy, pieces of pancreas no larger than 2 mm³ were fixed by immersion in a mixture of 2% glutaraldehyde in 0.1 M cacodylate buffer at pH 7.4. After postfixation in 1% osmium tetroxide and staining with 1% tannic acid and 1% uranyl acetate, tissue samples were dehydrated and embedded in Epon 812. Thin sections were counterstained with lead citrate and examined using a Philips CM 120 BioTwin transmission electron microscope (Philips Inc., Eindhoven, The Netherlands).

Induction of pancreatitis. Acute edematous pancreatitis was induced as described previously (26). In short, syncollin-deficient mice and littermate controls received seven intraperitoneal injections of the amphibian CCK-8 analogue caerulein (50 μ g/kg of body weight) at 1-h intervals. Animals were sacrificed at different time intervals (6, 12, 18, and 36 h and 7 days) after the injections. Untreated syncollin-deficient mice and wild-type littermates served as the control. At the given time points, serum samples of at least six animals in each group were analyzed. Light and electron microscopical analyses were performed on tissue samples from three and two animals, respectively, in each group.

Subcellular fractionation. Zymogen granules from pancreas were prepared as described previously (27). To enrich for membrane proteins, phase partitioning in Triton X-114 was performed on homogenate fractions (6). For immunoblotting with antibodies specific for syntaxin 2, syntaxin 3, syntaxin 4, and Rab3D, an aliquot of the detergent phase corresponding to 200 μ g of protein of the starting homogenate, and for SCAMP and synaptobrevin 2, aliquots corresponding to 50 μ g of protein of the starting homogenate, were loaded per lane (see Table 2). For immunoblotting with antibodies specific for GDP dissociation inhibitor, rabphilin, syncollin, PDI, calreticulin, BiP, and β -tubulin, 20 μ g of homogenate was loaded per lane. Signals were quantified using ECL reagent (NEN, Boston, Mass.) and Image Reader LAS-1000 in combination with AIDA software (ray-test).

For isopycnic sucrose density gradient centrifugation, zymogen granules were prepared as described previously (27). Zymogen granules derived from one pancreas were resuspended in 300 μ l of homogenization buffer (280 mM sucrose–5 mM morpholineethanesulfonic acid [pH 6.5]–1 mM EDTA–0.1 mM phenylmethylsulfonyl fluoride [PMSF]–10- μ g/ml soybean trypsin inhibitor–1- μ g/ml pepstatin–11- μ g/ml benzamide–1- μ g/ml antipain–1- μ g/ml leupeptin), loaded on top of a continuous sucrose gradient (10 ml of 35 to 60% [wt/vol] sucrose in 5 mM morpholineethanesulfonic acid [pH 6.5]–1 mM EDTA–0.1 mM PMSF–1- μ g/ml soybean trypsin inhibitor–0.1- μ g/ml pepstatin–1.1- μ g/ml benzamide–0.1- μ g/ml antipain–0.1- μ g/ml leupeptin) and centrifuged for 19 h at 40,000 rpm in a Beckman (Fullerton, Calif.) SW41 rotor. After centrifugation, fractions of 300 μ l were collected. All samples were analyzed for amylase (by enzyme assay; see below) and for SCAMP and synaptobrevin 2 (by immunoblotting). The sucrose concentration of each fraction was determined by refractometry.

Secretion of amylase. Secretion was monitored by measuring the release of amylase from pancreatic lobules (prepared as described in reference 38) in response to carbamylcholine. For each incubation, 20 to 30 lobules were suspended in oxygen-saturated incubation buffer consisting of 20 mM HEPES (pH 7.4), 120 mM NaCl, 5 mM KCl, 1.2 mM MgCl₂, 2 mM CaCl₂, 14 mM glucose, Eagle's minimal essential medium amino acid supplement, and 2 mM L-glutamine. Amylase discharge into the incubation medium was expressed as a percentage of the total amylase content in the lobules at the beginning of the incubation.

Protein synthesis and transport. Protein synthesis was measured as described previously (33) using 50 μ Ci of [³H]-labeled instead of [¹⁴C]-labeled amino acids (TRK440, Amersham)/ml and PMSF and soybean trypsin inhibitor as protease inhibitors in the lysis buffer. To measure the discharge of radioactively labeled proteins, lobules were incubated for 5 min in 500 μ Ci of [³H]-labeled amino acids/ml, washed, and transferred into unlabeled medium. Where indicated, the medium contained 0.5 μ M carbachol. At the indicated time points, aliquots of medium and lobules were removed, and the lobules were homogenized as described. Protein synthesis was measured by determination of trichloroacetic acid-insoluble radioactivity, and homogenate samples were normalized to the DNA content. The discharge of labeled protein was measured by quantifying the trichloroacetic acid-insoluble radioactivity of the medium. In all cases, radioactivity was determined by liquid scintillation counting. In all experiments, lactate dehydrogenase released into the medium remained constant during incubation time, showing that protein release is not caused by nonspecific tissue damage.

Other methods. Trypsin was measured after activation by enterokinase (38) as described in reference 22 using *N*-benzoyl arginine ethyl ester as the substrate. Chymotrypsin was assayed after activation by trypsin using benzoyl tyrosine ethyl ester as the substrate (22). Amylase was measured as described in reference 5, and lactate dehydrogenase was measured as described in reference 4. Protein was measured using the bicinchoninic acid method (Pierce) following the instructions of the manufacturer. All enzyme activities were normalized to DNA content (determined as described in reference 34) of the homogenate.

RESULTS

A murine genomic library was screened with rat syncollin cDNA as a probe to isolate genomic clones of the murine syncollin locus. Two independent clones were isolated which contain the two coding exons of mouse syncollin. The translated amino acid sequence of mouse syncollin is 86.6% identical to that of the rat and 73.7% identical to the human sequence (Fig. 1A).

The targeting vector for homologous recombination re-

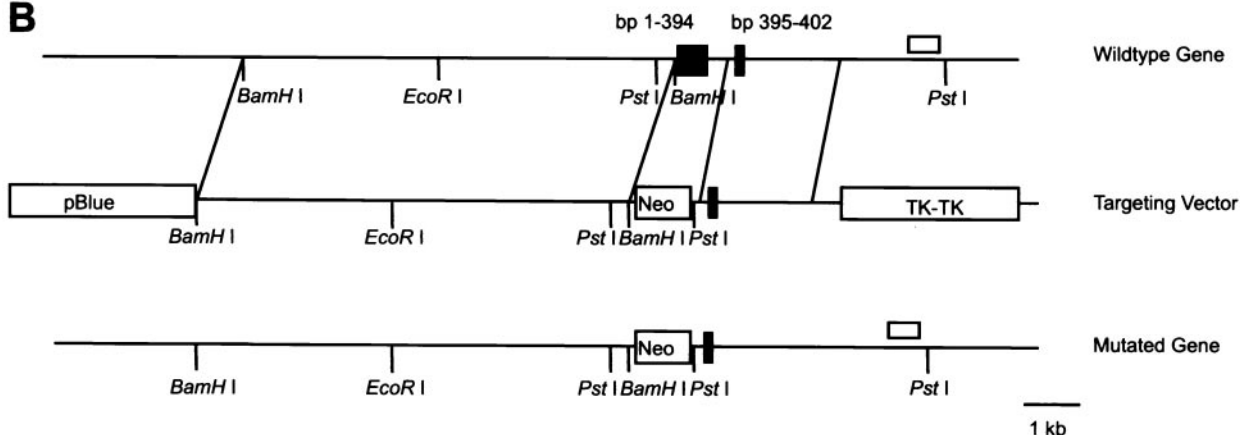
A

```

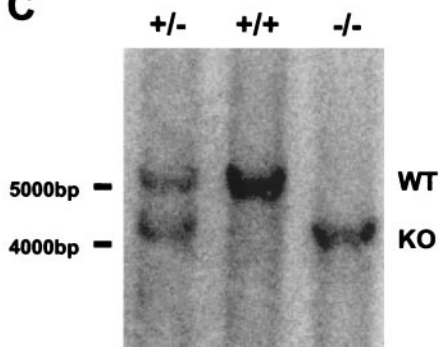
rat   MSPLCLLLLALALVAVPGAR GACVPADLKKSDGTRTCARLYE NSDPYYDNCCQGP ELSVDPGTDLP 67
mouse MSLLCPLLLLALALVAVPGAHGNCPVPADLKKSDGTRTCARLYEKSDPYYDNCCQGP VLSVEPGTDLP 67
human MSPLRPLLLLALALASVPCAQOGACFASADLKHSDGTRTCARLYDKSDPYYENCCGGAELSL ESGADLP 67

rat   YLPSDWSNSASSLVVAQRCELTVWVSLPGKR GKTRKFS TGSYPRLEEYRKGFIFGTWAKSISGLYCKCY 134
mouse YLPSGWSNTASSLVVGORCEITVWVSLPGKHGKTRKFTAGSYPRLEEYRKGFIFGDWSDSISALYCKCY 134
human YLPSNWNANTASSLVVAFRCELTVWVSRQKAGKTHKFSAGTYPRLEEYRRGILGDWSNAISALYCRCS 134
    
```

B



C



D

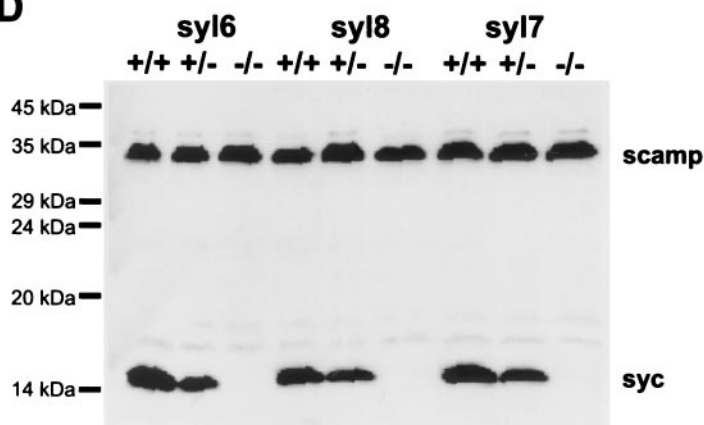


FIG. 1. (A) Syncollin is conserved in mammals. A sequence comparison of syncollin derived from rat, mouse, and human is shown. Sequence alignment was performed using the programs ClustalW and Boxshade. Identical and conserved amino acids are darkly and lightly shaded, respectively. (B) Gene targeting of syncollin. Maps of the wild-type syncollin gene, the respective targeting vector, and the resulting mutant gene are shown. Positions of exons (black boxes with base pairs of corresponding cDNA) and restriction enzyme sites are indicated. The positions of the probe to identify wild-type and mutant alleles are indicated by open bars. Neo, neomycin resistance gene; TK, thymidine kinase gene. (C) Southern blot analysis of deletion mutations. Mouse tail DNA from adult wild-type (+/+) mice and mice heterozygous (+/-) or homozygous (-/-) for the mutation in syncollin genes were analyzed as described in Materials and Methods. Positions of wild-type (WT) and mutant (KO) alleles are indicated. (D) Syncollin expression in mice. Zymogen granules (20 µg/lane) from adult wild-type (+/+) mice and heterozygous (+/-) or homozygous (-/-) mice derived from three independent stem cell clones (syl6, syl8, and syl7) were analyzed by sodium dodecyl sulfate-polyacrylamide gel electrophoresis and immunoblotting using antibodies specific for SCAMP as a marker for zymogen granules and syncollin (sync).

placed exon 1 (coding for residues 1 to 132 of syncollin) by a neomycin resistance cassette (Fig. 1B). Electroporation of the targeting vector into E14.1 mouse embryonic stem cells (20) resulted in nine independent clones in which homologous re-

combination of the syncollin gene had occurred. Highly chimeric mice were generated by blastocyst injection using three independent embryonic stem cell clones. These mice were used for breeding to generate heterozygous mutant mice. Inter-

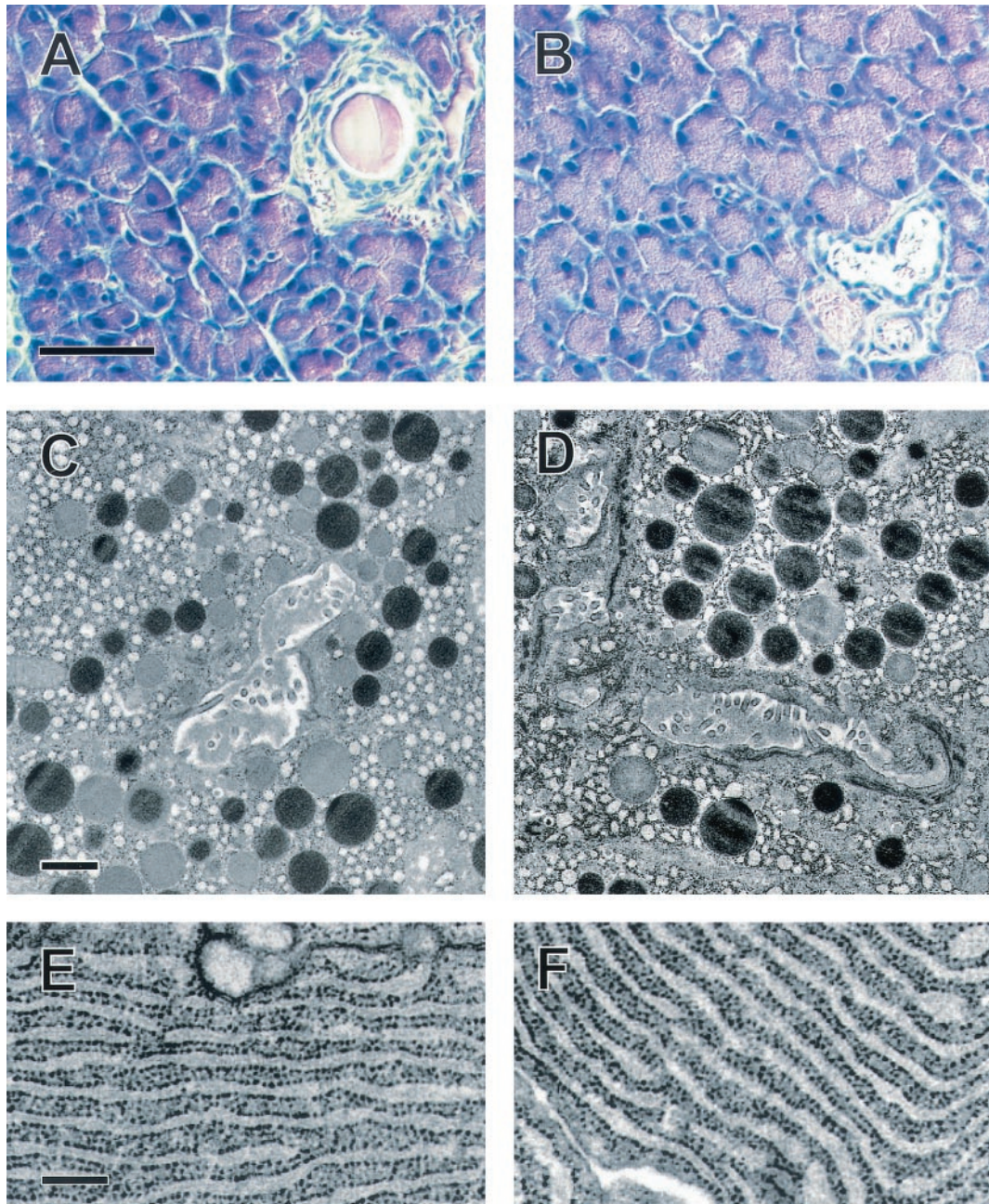


FIG. 2. The structure of the pancreas at the light and electron microscopy level is normal in syncollin-deficient mice. (A and B) Micrographs of pancreatic sections, stained with hematoxylin and eosin, that were obtained from 90-day-old wild-type (A) and syncollin-deficient (B) mice. The pancreatic morphology is normal. Bars, 50 μ m. (C to F) Electron micrographs obtained from thin sections of pancreas derived from wild-type (C and E) and syncollin-deficient mice (D and F) show no difference in acinar cell differentiation and zymogen granules (C and D; bars, 1 μ m) or in morphology of the endoplasmic reticulum (E and F; bars, 250 nm).

breeding of the heterozygous mice resulted in offspring that showed the predicted Mendelian frequencies of wild-type, heterozygous, and homozygous genotypes. When pancreas homogenates (not shown) or preparations of pancreatic zymogen granules obtained from adult mice were analyzed by immunoblotting (Fig. 1D), no trace of syncollin expression was detected in homozygous mutants. In granule preparations obtained from heterozygous animals, protein levels of syncollin were reduced with respect to wild-type expression levels.

Mice lacking syncollin were viable and fertile and exhibited no obvious phenotypical changes. Mutant mice were capable of reproducing and of caring for their offspring. Their body weights and their life spans were comparable to those of their wild-type and heterozygous littermates.

To determine whether the exocrine pancreas is altered in syncollin-deficient mice, we first performed a morphological analysis. Hematoxylin and eosin staining of pancreatic sections obtained from 90-day-old homozygous mutant mice showed

TABLE 1. Protein and enzyme levels in the pancreas of wild-type (+/+), heterozygous (+/-), and homozygous (-/-) mice^a

Genotype	% (range) of:			
	Protein	Chymotrypsin	Trypsin	Amylase
+/+	100 (91–109)	100 (94–109)	100 (89–108)	100 (86–110)
+/-	100 (96–111)	98 (90–113)	100 (92–114)	95 (84–105)
-/-	105 (98–112)	104 (95–112)	107 (98–113)	105 (92–118)

^a Protein levels and enzyme activities were normalized to DNA content. Four mice of each genotype were analyzed. The means of wild-type values were set to 100%.

normal acinar morphology with no sign of tissue inflammation (Fig. 2B). Furthermore, no change in morphology was observed during weaning or in animals older than 1 year (data not shown). Examination by electron microscopy showed normally organized acini (Fig. 2D). Abundance and average size of zymogen granules were similar in acinar cells of syncollin-deficient mice and littermate controls. Furthermore, morphology of the endoplasmic reticulum is unchanged in syncollin-deficient mice (Fig. 2E and F). In addition, zymogen granules were purified, and their buoyant density was compared using isopycnic sucrose density gradient centrifugation. No difference was found between syncollin-deficient mice and littermate controls (data not shown), suggesting that the granular protein concentration is unaltered in syncollin-deficient mice.

Consistent with the normal morphology, we found that in syncollin-deficient mice the overall protein content of the pancreas was unchanged. Similarly, no change was observed in the pancreatic levels of chymotrypsin, trypsin, and amylase (Table 1) and in the serum levels of amylase and lactate dehydrogenase (data not shown). Furthermore, we examined the levels of several proteins known to be involved in vesicular trafficking of zymogen granules. Again, no difference was observed between wild-type and syncollin-deficient mice (Table 2). Also, in agreement with the unchanged morphology of the endoplasmic reticulum, the expression levels of several chaperons known to

TABLE 2. Levels in pancreatic tissue of syncollin, tubulin, chaperons of the endoplasmic reticulum, and several trafficking proteins^a

Protein	% (range) of protein for genotype:	
	+/+	-/-
SNAP-23	100 (96.6–102.6)	96.4 (87.6–100.9)
Synaptobrevin 2	100 (94.3–105.9)	94.2 (89.2–98.7)
Syntaxin 2	100 (98.8–102.3)	100.9 (93.5–106.7)
Syntaxin 3	100 (97.5–101.8)	101.2 (97.7–103.7)
Syntaxin 4	100 (96.8–105.4)	101.2 (97.0–104.4)
SCAMP	100 (96.9–103.1)	102.6 (96.9–107.4)
GDI	100 (94.9–108.7)	101.2 (100.8–103.0)
Rab3D	100 (92.3–112.2)	93.7 (90.9–96.4)
Rabphilin	100 (91.1–108.4)	102.8 (101.5–104.6)
Calreticulin	100 (98.1–103.1)	103.9 (100.8–109.8)
PDI	100 (95.7–104.0)	94.9 (90.7–99.8)
BiP	100 (93.8–109.4)	103.6 (90.5–113.6)
Syncollin	100 (97.8–103.0)	0.7 (0.2–1.0)
β-Tubulin	100 (94.4–103.5)	93.9 (84.5–102.3)

^a Pancreatic proteins derived from wild-type (+/+) and knockout (-/-) mice (three mice per group) were analyzed by sodium dodecyl sulfate-polyacrylamide gel electrophoresis and quantitative immunoblotting. Signals were normalized to the average of signals for wild-type mice and given in percentages.

reside in the lumen of the endoplasmic reticulum (PDI, calreticulin, and BiP) are unchanged (Table 2).

The experiments described so far did not reveal any difference between wild-type and syncollin-deficient mice with respect to pancreas morphology and protein content. Next, we examined whether the organ would also behave normally under stress. For this purpose, we treated the mice with caerulein according to a protocol that is well established for inducing self-limiting acute pancreatitis. Caerulein was repeatedly applied by intraperitoneal injection at a supramaximal dose. At different time points after the onset of the treatment, animals were sacrificed and analyzed both for morphological alterations of the pancreas and for serum levels of pancreatic amylase and lactate dehydrogenase. Acute pancreatitis in wild-type mice is characterized by mild edema 6 to 12 h after induction (Fig. 3A and C), followed by acinar vacuolization and single-cell necrosis 12 to 18 h after induction (C and E). Furthermore, we observed tissue inflammation starting 12 h after induction of acute pancreatitis. Based on morphological evaluation, syncollin-deficient mice show a more severe course of acute pancreatitis than wild-type mice (Fig. 3B, D, and F). This was evidenced by pronounced intralobular edema starting already 6 h after induction (Fig. 3B) and by marked vacuolization 12 h after induction (Fig. 3D). Furthermore, marked acinar cell necrosis was observed already 12 h after induction (Fig. 3D). Fig. 3F shows extensive pancreatic necrosis that involves up to 75% of the organ 18 h after induction in syncollin-deficient mice. Furthermore, interstitial inflammation was still evident in knockout animals 36 h after induction (Fig. 3H), while wild-type controls had largely recovered and showed only minor alterations of the pancreatic morphology (Fig. 3G). These data indicate that syncollin-deficient mice are more susceptible to caerulein-induced pancreatitis. Furthermore, regeneration appears to be delayed in the knockout animals. Seven days after induction of acute pancreatitis, both syncollin-deficient mice and wild-type controls display normal morphology, indicating that despite the more severe course of the pancreatitis in syncollin-deficient mice, the pancreas retained its ability for complete regeneration.

Serum amylase levels showed a similar pattern in both wild-type and syncollin-deficient mice during the course of the pancreatitis, with a maximum 12 h after induction (Fig. 4A). The tissue amylase content (Fig. 4B) mirrored the levels of serum amylase, showing a minimum 12 h after induction. As expected, regeneration of the pancreas is accompanied by an increase in pancreatic amylase and a decrease of serum amylase levels. No major differences were observed between wild-type and syncollin-deficient mice, although slight changes were evident. First, 18 h after induction, serum amylase levels appeared to be somewhat higher in knockout than in wild-type animals. Furthermore, 36 h after induction, pancreatic amylase levels were still decreased in syncollin-deficient mice whereas wild-type levels had returned to normal values (Fig. 4B). This delay is consistent with the morphological findings described above. Seven days after induction, serum and pancreatic amylase levels were normal, again in good agreement with the morphological observations.

Together, the experiments described above uncovered a defect in the function of the pancreas of syncollin-deficient mice that was not obvious under normal physiological conditions.

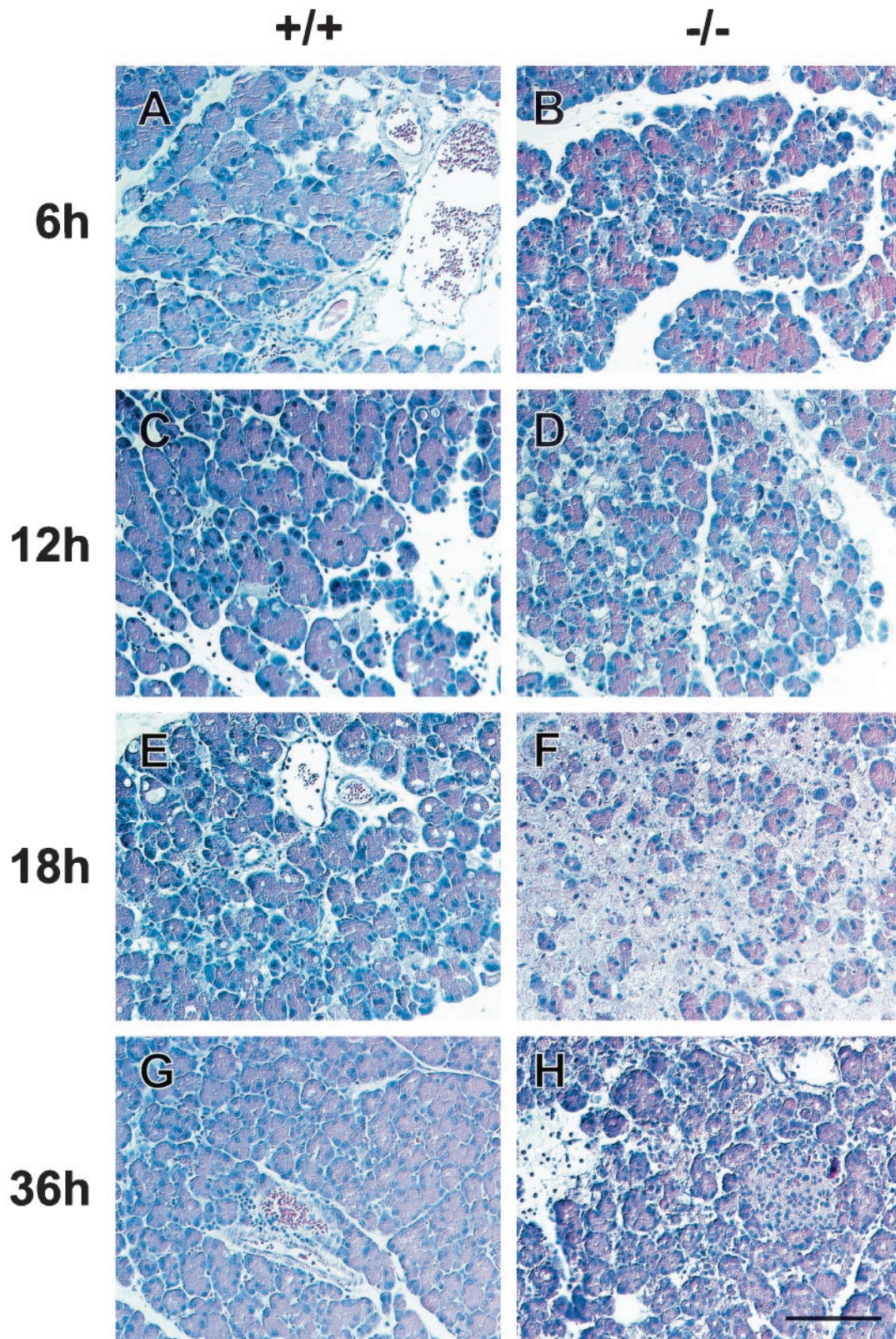


FIG. 3. Damage of the pancreas after induction of acute pancreatitis is more severe in syncollin-deficient mice than in wild-type littermates. The figure shows micrographs of pancreatic sections, stained with hematoxylin and eosin, obtained from wild-type (A, C, E, and G) and syncollin-deficient (B, D, F, and H) mice 6 h (A and B), 12 h (C and D), 18 h (E and F), and 36 h (G and H) after induction. Bar, 100 μ m.

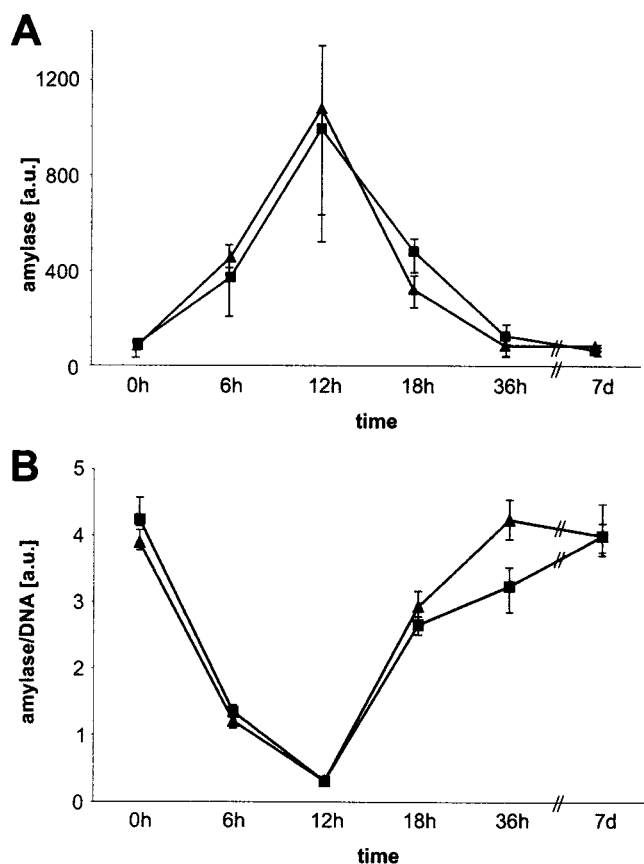


FIG. 4. Time course of serum (A) and tissue (B) amylase levels of wild-type (triangles) and knockout (squares) animals after induction of acute pancreatitis. The values are means for six (A) and four (B) animals, and the bars indicate the range of the data points. Tissue amylase was normalized to DNA content.

Since syncollin is specifically localized to the luminal side of the zymogen granule membrane, we investigated in more detail whether one or more steps of the secretory pathway are altered in syncollin-deficient mice.

First, we evaluated whether secretagogue-induced secretion was changed. Pancreatic lobules were prepared, and amylase release was monitored in vitro using standard procedures (38). No differences were observed between wild-type and syncollin-deficient mice when secretion was stimulated by various concentrations of carbachol (Fig. 5A). Maximal secretion was observed at a carbachol concentration of 0.5 μ M. To exclude differences in the release kinetics, the time dependence of amylase release was monitored. As shown in Fig. 5B, no differences were found regardless of whether stimulation was conducted at submaximal (0.1 μ M) or maximal (0.5 μ M) carbachol concentrations. Furthermore, no differences were observed at various carbachol or cholecystokinin concentrations when isolated acini instead of lobules were used (data not shown). Together, these data argue against a direct role of syncollin in the stimulus-evoked exocytosis of mature zymogen granules.

Second, we measured protein synthesis by monitoring the incorporation of radiolabeled amino acids into total protein,

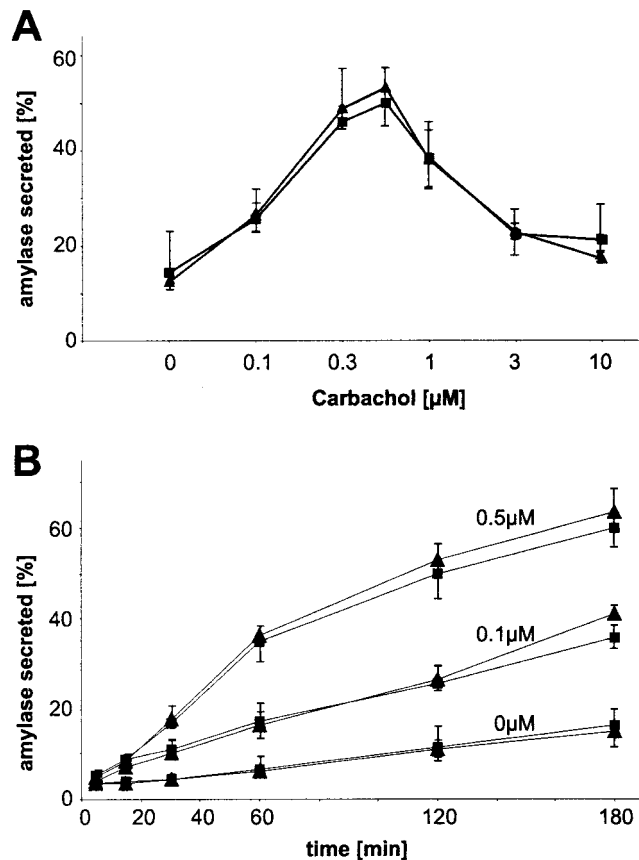


FIG. 5. Amylase release is normal in the pancreas of syncollin-deficient mice. Amylase release was measured using isolated pancreatic lobules prepared from wild-type (triangle) and knockout (squares) mice (four mice per group). Secretion is expressed as the percentage of amylase released into the medium with respect to the total amylase content (sum of amylase discharged into the medium and amylase retained in the tissue). Each value is the mean for the four independent experiments; bars indicate the range. (A) Dose dependence of carbachol-induced amylase release. (B) Discharge kinetics of amylase in response to 0.5 and 0.1 μ M carbachol.

again using isolated pancreatic lobules as an in vitro model. Pancreatic lobules were incubated in the presence of radioactively labeled amino acids. At different time points lobules were removed, washed and homogenized. Protein was precipitated by trichloroacetic acid, and the amount of incorporated radioactivity was measured. As shown in Fig. 6, incorporation of radioactivity into protein was reduced by about 40% in syncollin-deficient mice. This reduction was observed regardless of whether incorporation was determined 30, 60, or 90 min after the onset of the incubation in the presence of labeled amino acids. These data document that syncollin-deficient mice exhibit a significantly reduced rate of protein synthesis.

Protein synthesis in the acinar cell is known to be influenced by the performance of the entire secretory pathway, including intracellular transport and exocytosis. Thus, the observed reduction in protein synthesis may be due not to a direct involvement of syncollin in protein synthesis but rather to a downstream step in the pathway. Since secretion itself is normal (Fig. 5), we investigated whether intracellular transport rates

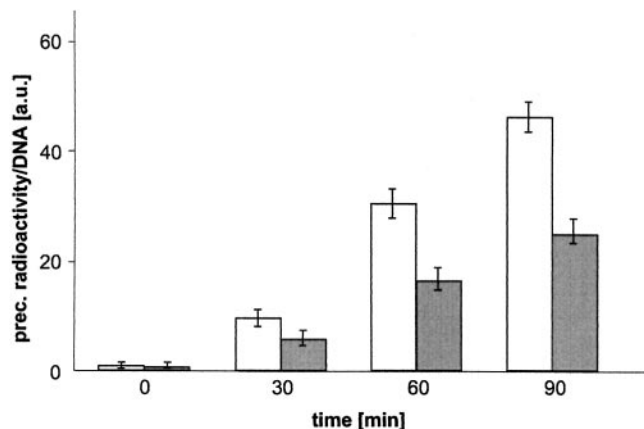


FIG. 6. Protein synthesis is reduced in the pancreas of syncollin-deficient mice. Pancreatic lobules derived from wild-type (white bars) and knockout (gray bars) mice (four mice per group) were incubated in medium containing ^3H -labeled amino acids. At the indicated time points an aliquot of the lobules was removed, washed, and homogenized. Trichloroacetic acid-precipitable (prec.) radioactivity and DNA concentration were determined. Protein synthesis is normalized to DNA content. Values (expressed in arbitrary units [a.u.]) are means for the four independent experiments; bars indicate the range.

of newly synthesized zymogens are affected, using pulse-chase experiments. Lobules were pulse labeled for 5 min with radioactive amino acids, washed, and transferred to unlabeled medium, followed by incubation in either the presence or absence of the secretagogue carbachol. At different time points, the amount of labeled protein was determined in the medium and in the tissue.

Basal secretion of the unstimulated controls was low in both wild-type and knockout mice (Fig. 7A). However, a significant difference was observed between wild-type and syncollin-deficient mice when secretion of labeled protein was observed in the presence of carbachol. In lobules prepared from wild-type mice, discharge of labeled proteins commenced 30 min after the pulse. In contrast, secretion of labeled proteins from lobules of syncollin-deficient mice was first measurable 60 min after the pulse. As expected, the tissue levels of radiolabeled proteins showed an inverse relationship. After reaching a plateau level, the tissue levels remained unchanged over the entire incubation period in unstimulated control incubations. In the carbachol-containing incubations, tissue levels started to decrease after 30 and 60 min in lobules prepared from wild-type and syncollin-deficient mice, respectively (Fig. 7B). Together these data show that the intracellular transit time of secretory proteins is significantly prolonged in syncollin-deficient mice.

DISCUSSION

In this study we have analyzed the role of syncollin by creating syncollin-deficient transgenic mice. Syncollin is not essential for viability. In addition, morphology, protein content, and release kinetics of the pancreas are not affected by the loss of the protein. However, syncollin-deficient mice reacted to caerulein hyperstimulation with a more severe pancreatitis. Furthermore, we found that the rates of both protein synthesis and intracellular transport of zymogens were reduced.

Syncollin is a small protein that is tightly associated with the

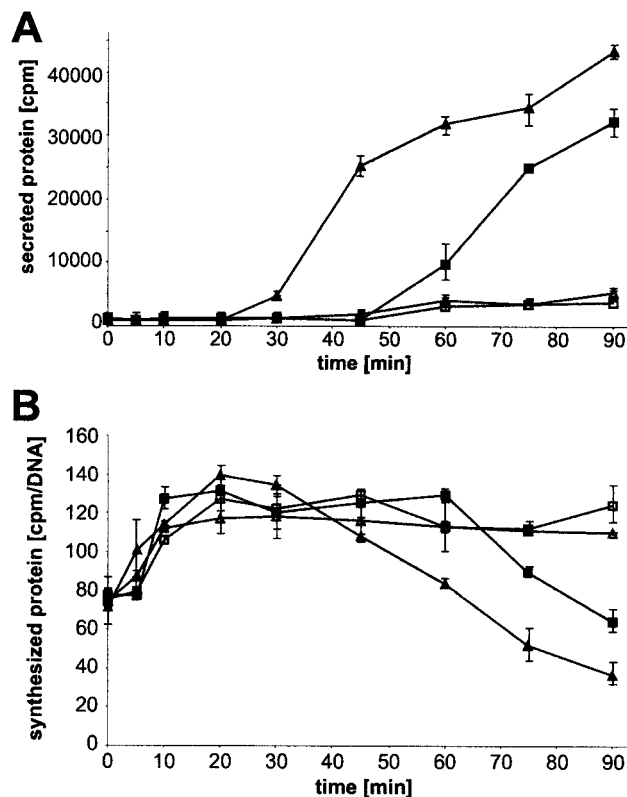


FIG. 7. Intracellular transport of proteins is slowed in syncollin-deficient mice. Pancreatic lobules derived from wild-type (triangle) and knockout (square) mice (two mice per group) were incubated for 5 min in medium containing ^3H -labeled amino acids. After a chase to cold medium containing either no stimulants (open symbols) or 0.5 μM carbachol (filled symbols), aliquots of the medium (A) and the lobules (B) were removed as indicated, and trichloroacetic acid-precipitable radioactivity was determined. In panel B, the values were normalized to the DNA content of the homogenates (see the legend to Fig. 6). Values are means for the two independent experiments; bars indicate the range.

luminal side of the zymogen granule membrane (2). In the membrane, the protein forms homo-oligomers that probably consist of six monomers (2, 19). Its expression appears to be largely restricted to the pancreas, where it is expressed at rather high levels (13). Recently it has been reported that syncollin mRNA is expressed in epithelial cells of the duodena of rats and furthermore that the expression levels are increased in response to feeding and during development (40). However, we were unable to detect syncollin protein in the duodena of adult mice. Furthermore, syncollin is conspicuously absent from other exocrine and protein-secreting endocrine glands, and no homologous proteins were found in extensive database searches (unpublished observations).

This unusual expression pattern suggests that the function of syncollin is specific for the pancreas, and therefore we have focused our analysis on this organ. Although the precise role of the protein remains to be elucidated, several conclusions can be drawn from our findings. First, it is clear that syncollin is not an essential factor for the basic functioning of the pancreatic acinar cell under normal conditions. In our comparative analysis of organs derived from wild-type and knockout mice, we

are unable to detect differences in sensitivity to secretagogues, acinar cell morphology at the light-microscopy and ultrastructural level, content in zymogens and trafficking proteins, and buoyant density of zymogen granules. These findings show that the secretory pathway in mutant mice is capable of equipping the acinar cell with a normal load of fully charged zymogen granules in the absence of syncollin. Furthermore, we found no abnormalities in cell polarity or in the capacity of the acinar cell to undergo exocytosis at normal rates. Second, the significant reductions in the rates of protein synthesis and intracellular transport reveal a defect in the efficiency of zymogen synthesis and/or transport and packaging. Despite the normal morphological and functional parameters, it is thus possible that under certain physiological conditions these reduced synthesis and transport rates affect the overall performance of the organ. For instance, it is conceivable that the organ cannot keep up with zymogen replenishment under extended and strong stimulatory conditions. Furthermore, the fact that the organ reacts more severely to caerulein overstimulation may be related to the decrease in synthesis and transport rates. Thus, the defect in the secretory pathway can negatively affect organ function *in vivo* under certain conditions. Despite recent progress, the precise sequence of events leading from hyperstimulation of the CCK_A receptors to the disintegration of acinar cells is unknown. Supramaximal doses of caerulein induce a sustained increase of intracellular calcium levels and a block of apical exocytosis. The first steps of autodigestion involve redistribution of cathepsin B from lysosomes to zymogen granules and trypsin activation, followed by acinar cell necrosis and tissue inflammation. The enhancement of these symptoms in syncollin-deficient mice suggests that even mild defects of the secretory pathway may negatively affect the course and outcome of acute pancreatitis.

Currently it is not possible to pinpoint the precise molecular steps that are affected by the lack of syncollin and that give rise to the deficiencies in protein synthesis and intracellular transport. Thus, it remains to be established which of the reduced parameters are primarily caused by the lack of syncollin and which of them are secondary to the primary defect. However, some educated guesses can be made. For instance, we don't believe that syncollin functions directly in protein biosynthesis as a pancreas-specific accelerator of synthesis rates. Pancreatic synthesis rates are known to be reduced under a variety of adverse conditions, such as energy depletion (42) and a block in secretion or intracellular transport (25, 47). Syncollin is specifically localized to the lumen of the zymogen granule membrane (2), whereas it would need to operate in the rough endoplasmic reticulum if it were involved in controlling protein synthesis rates. Rather, we regard it as more likely that syncollin increases the efficiency of protein maturation and/or packaging at a later state of the secretory pathway, for instance during the formation of condensing vacuoles and/or the maturation of secretory granules. It is possible that syncollin forms a partially redundant functional network with other proteins (e.g., GP-2 [36] or other granule membrane proteins, such as ZG16 [23]) that may function in the organization of the granule interior at various stages of maturation. Since the pancreas exhibits the highest rates of protein synthesis and processing of all organs in the body, it may require tissue-specific factors

such as syncollin in order to achieve such exceptional biosynthetic competence.

ACKNOWLEDGMENTS

We thank the staff of the animal core facilities at the Max-Planck Institute for Experimental Medicine and Max-Planck Institute for Biophysical Chemistry for invaluable help with blastocyst injection and animal husbandry. We are grateful to H. F. Kern and J. M. Edwardson as well as members of N. Brose's and R. Jahn's lab for useful comments and critical discussions.

REFERENCES

- Altschul, S. F., T. L. Madden, A. A. Schaffer, J. Zhang, Z. Zhang, W. Miller, and D. J. Lipman. 1997. Gapped BLAST and PSI-BLAST: a new generation of protein database search programs. *Nucleic Acids Res.* **25**:3389–3402.
- An, S. J., N. J. Hansen, A. Hodel, R. Jahn, and J. M. Edwardson. 2000. Analysis of the association of syncollin with the membrane of the pancreatic zymogen granule. *J. Biol. Chem.* **275**:11306–11311.
- Arvan, P., and D. Castle. 1998. Sorting and storage during secretory granule biogenesis: looking backward and looking forward. *Biochem. J.* **332**:593–610.
- Bergmeyer, H. U. 1974. *Methoden der enzymatischen Analyse*. Verlag Chemie, Weinheim/Bergstrasse, Germany.
- Bernfeld, P. 1955. Amylase, alpha and beta. *Methods Enzymol.* **1**:31149–31158.
- Bordier, C. 1981. Phase separation of integral membrane proteins in Triton X-114 solution. *J. Biol. Chem.* **256**:1604–1607.
- Brand, S. H., S. M. Laurie, M. B. Mixon, and J. D. Castle. 1991. Secretory carrier membrane proteins 31–35 define a common protein composition among secretory carrier membranes. *J. Biol. Chem.* **266**:18949–18957.
- Case, R. M. 1978. Synthesis, intracellular transport and discharge of exportable proteins in the pancreatic acinar cell and other cells. *Biol. Rev. Camb. Philos. Soc.* **53**:211–354.
- Chou, J. H., and R. Jahn. 2000. Binding of Rab3A to synaptic vesicles. *J. Biol. Chem.* **275**:9433–9440.
- Cronshagen, U., P. Volland, and H. F. Kern. 1994. cDNA cloning and characterization of a novel 16 kDa protein located in zymogen granules of rat pancreas and goblet cells of the gut. *Eur. J. Cell Biol.* **65**:366–377.
- De Lisle, R. C. 1994. Characterization of the major sulfated protein of mouse pancreatic acinar cells: a high molecular weight peripheral membrane glycoprotein of zymogen granules. *J. Cell. Biochem.* **56**:385–396.
- Edelmann, L., P. I. Hanson, E. R. Chapman, and R. Jahn. 1995. Synaptobrevin binding to syntaxin: a potential mechanism for controlling the exocytotic fusion machine. *EMBO J.* **14**:224–231.
- Edwardson, J. M., S. An, and R. Jahn. 1997. The secretory granule protein syncollin binds to syntaxin in a Ca²⁺(+)-sensitive manner. *Cell* **90**:325–333.
- Fasshauer, D., W. Antonin, M. Margittai, S. Pabst, and R. Jahn. 1999. Mixed and non-cognate SNARE Complexes. Characterization of assembly and biophysical properties. *J. Biol. Chem.* **274**:15440–15446.
- Gaisano, H. Y., M. Ghai, P. N. Malkus, L. Sheu, A. Bouquillon, M. K. Bennett, and W. S. Trimble. 1996. Distinct cellular locations of the syntaxin family of proteins in rat pancreatic acinar cells. *Mol. Biol. Cell* **7**:2019–2027.
- Gaisano, H. Y., L. Sheu, J. K. Foskett, and W. S. Trimble. 1994. Tetanus toxin light chain cleaves a vesicle-associated membrane protein (VAMP) isoform 2 in rat pancreatic zymogen granules and inhibits enzyme secretion. *J. Biol. Chem.* **269**:17062–17066.
- Gaisano, H. Y., L. Sheu, G. Grondin, M. Ghai, A. Bouquillon, A. Lowe, A. Beaudoin, and W. S. Trimble. 1996. The vesicle-associated membrane protein family of proteins in rat pancreatic and parotid acinar cells. *Gastroenterology* **111**:1661–1669.
- Hansen, N. J., W. Antonin, and J. M. Edwardson. 1999. Identification of SNAREs involved in regulated exocytosis in the pancreatic acinar cell. *J. Biol. Chem.* **274**:22871–22876.
- Hodel, A., S. J. An, N. J. Hansen, J. Lawrence, B. Wasle, M. Schrader, and J. M. Edwardson. 2001. Cholesterol-dependent interaction of syncollin with the membrane of the pancreatic zymogen granule. *Biochem. J.* **356**:843–850.
- Hooper, M., K. Hardy, A. Handyside, S. Hunter, and M. Monk. 1987. HPRT-deficient (Lesch-Nyhan) mouse embryos derived from germline colonization by cultured cells. *Nature* **326**:292–295.
- Hoops, T. C., I. Ivanov, Z. Cui, V. Colomer-Gould, and M. J. Rindler. 1993. Incorporation of the pancreatic membrane protein GP-2 into secretory granules in exocrine but not endocrine cells. *J. Biol. Chem.* **268**:25694–25705.
- Hummel, B. C. 1959. A modified spectrophotometric determination of chymotrypsin, trypsin and thrombin. *Can. J. Biochem.* **37**:1393–1399.
- Kleene, R., H. Dartsch, and H. F. Kern. 1999. The secretory lectin ZG16p mediates sorting of enzyme proteins to the zymogen granule membrane in pancreatic acinar cells. *Eur. J. Cell Biol.* **78**:79–90.
- Köhler, G., and C. Milstein. 1975. Continuous cultures of fused cells secreting antibody of predefined specificity. *Nature* **256**:495–497.
- Koike, H., M. L. Steer, and J. Meldolesi. 1982. Pancreatic effects of ethi-

- onine: blockade of exocytosis and appearance of crinophagy and autophagy precede cellular necrosis. *Am. J. Physiol.* **242**:G297–G307.
26. **Lampel, M., and H. F. Kern.** 1977. Acute interstitial pancreatitis in the rat induced by excessive doses of a pancreatic secretagogue. *Virchows Arch. A (Pathol. Anat. Histol.)* **373**:97–117.
 27. **Nadin, C. Y., J. Rogers, S. Tomlinson, and J. M. Edwardson.** 1989. A specific interaction in vitro between pancreatic zymogen granules and plasma membranes: stimulation by G-protein activators but not by Ca²⁺. *J. Cell Biol.* **109**:2801–2808.
 28. **Ohnishi, H., S. A. Ernst, N. Wys, M. McNiven, and J. A. Williams.** 1996. Rab3D localizes to zymogen granules in rat pancreatic acini and other exocrine glands. *Am. J. Physiol.* **271**:G531–G538.
 29. **Ohnishi, H., T. Mine, H. Shibata, N. Ueda, T. Tsuchida, and T. Fujita.** 1999. Involvement of Rab4 in regulated exocytosis of rat pancreatic acini. *Gastroenterology* **116**:943–952.
 30. **Ohnishi, H., L. C. Samuelson, D. I. Yule, S. A. Ernst, and J. A. Williams.** 1997. Overexpression of Rab3D enhances regulated amylase secretion from pancreatic acini of transgenic mice. *J. Clin. Investig.* **100**:3044–3052.
 31. **Palade, G.** 1975. Intracellular aspects of the process of protein synthesis. *Science* **189**:347–358.
 32. **Petersen, C. C., E. C. Toescu, and O. H. Petersen.** 1991. Different patterns of receptor-activated cytoplasmic Ca²⁺ oscillations in single pancreatic acinar cells: dependence on receptor type, agonist concentration and intracellular Ca²⁺ buffering. *EMBO J.* **10**:527–533.
 33. **Rausch, U., P. Vasiloudes, K. Rudiger, and H. F. Kern.** 1985. In-vivo stimulation of rat pancreatic acinar cells by infusion of secretin. I. Changes in enzyme content, pancreatic fine structure and total rate of protein synthesis. *Cell Tissue Res.* **242**:633–639.
 34. **Richards, G. M.** 1974. Modifications of the diphenylamine reaction giving increased sensitivity and simplicity in the estimation of DNA. *Anal. Biochem.* **57**:369–376.
 35. **Ronzio, R. A., K. E. Kronquist, D. S. Lewis, R. J. MacDonald, S. H. Mohrlök, and J. J. O'Donnell, Jr.** 1978. Glycoprotein synthesis in the adult rat pancreas. IV. Subcellular distribution of membrane glycoproteins. *Biochim. Biophys. Acta* **508**:65–84.
 36. **Scheele, G. A., S. Fukuoka, and S. D. Freedman.** 1994. Role of the GP2/THP family of GPI-anchored proteins in membrane trafficking during regulated exocrine secretion. *Pancreas* **9**:139–149.
 37. **Scheele, G. A., and H. F. Kern.** 1993. Cellular compartmentation, protein processing, and secretion in exocrine pancreas, p. 121–150. *In* V. L. Go (ed.) et al., *The pancreas: biology, pathobiology, and disease*, 2nd edition. Raven Press, New York, N.Y.
 38. **Scheele, G. A., and G. E. Palade.** 1975. Studies on the guinea pig pancreas. Parallel discharge of exocrine enzyme activities. *J. Biol. Chem.* **250**:2660–2670.
 39. **Schlüter, O. M., E. Schnell, M. Verhage, T. Tzonopoulos, R. A. Nicoll, R. Janz, R. C. Malenka, M. Geppert, and T. C. Südhof.** 1999. Rabphilin knock-out mice reveal that rabphilin is not required for rab3 function in regulating neurotransmitter release. *J. Neurosci.* **19**:5834–5846.
 40. **Tan, S., and S. C. Hooi.** 2000. Syncollin is differentially expressed in rat proximal small intestine and regulated by feeding behavior. *Am. J. Physiol.* **278**:G308–G320.
 41. **Thomas, K. R., and M. R. Capecchi.** 1987. Site-directed mutagenesis by gene targeting in mouse embryo-derived stem cells. *Cell* **51**:503–512.
 42. **Tooze, J., H. F. Kern, S. D. Fuller, and K. E. Howell.** 1989. Condensation-sorting events in the rough endoplasmic reticulum of exocrine pancreatic cells. *J. Cell Biol.* **109**:35–50.
 43. **Tooze, S. A.** 1998. Biogenesis of secretory granules in the trans-Golgi network of neuroendocrine and endocrine cells. *Biochim. Biophys. Acta* **1404**:231–244.
 44. **Valentijn, J. A., L. T. Gien, K. M. Valentijn, and J. D. Jamieson.** 2000. An evaluation of the expression, subcellular localization, and function of rab4 in the exocrine pancreas. *Biochem. Biophys. Res. Commun.* **268**:847–852.
 45. **Valentijn, J. A., F. D. Gumkowski, and J. D. Jamieson.** 1996. The expression pattern of rab3D in the developing rat exocrine pancreas coincides with the acquisition of regulated exocytosis. *Eur. J. Cell Biol.* **71**:129–136.
 46. **Wagner, A. C., M. Z. Strowski, and J. A. Williams.** 1994. Identification of Rab 5 but not Rab 3A in rat pancreatic zymogen granule membranes. *Biochem. Biophys. Res. Commun.* **200**:542–548.
 47. **Waschulewski, I. H., M. L. Kruse, B. Agricola, H. F. Kern, and W. E. Schmidt.** 1996. Okadaic acid disrupts Golgi structure and impairs enzyme synthesis and secretion in the rat pancreas. *Am. J. Physiol.* **270**:G939–G947.